Virus Research 269 (2019) 197639

Contents lists available at ScienceDirect

Virus Research

journal homepage: www.elsevier.com/locate/virusres

Short communication

Two mutations in viral protein enhance the adaptation of waterfowl-origin H3N2 virus in murine model

Zhijun Yu[a,*], Kaihui Cheng[d], Tiecheng Wang[b], Zhiguang Ren[e], Jiaqiang Wu[a], Hongbin He[c], Yuwei Gao[b,**]

[a] Institute of Poultry Science, Shandong Academy of Agricultural Sciences, Jinan, 250023, China
[b] Key Laboratory of Jilin Province for Zoonosis Prevention and Control, Military Veterinary Research Institute, Academy of Military Medical Sciences, Changchun, 130122, China
[c] College of Life Sciences, Shandong Normal University, Jinan, 250014, China
[d] Dairy Cattle Research Center, Shandong Academy of Agricultural Sciences, Jinan, 250132, China
[e] Joint National Laboratory for Antibody Drug Engineering, Henan University, School of Basic Medical Sciences, Kaifeng, 475004, China

ARTICLE INFO

Keywords:
H3N2
Avian influenza virus
Waterfowl
Mice
Pathogenesis

ABSTRACT

After serial passage of a waterfowl-origin H3N2 subtype avian influenza virus in BALB/c mice, we obtained H3N2 mouse-adapted variants and identified eight amino acid substitutions in five viral proteins in our previous study. Here, we analyze the key mutations determining viral pathogenicity in mammals. We found that both PB2-D701N mutation and M1-M192V mutation were implicated in the viral pathogenic phenotypic variation of H3N2 avian influenza virus in mice. Furthermore, we found that PB2-D701N could enhance viral replication *in vitro* and *in vivo* and expanded viral tissue tropism. Our data suggest that PB2-D701N and M1-M192V are the virulence markers of H3N2 avian influenza virus, and these markers can be used in the trans-species transmission surveillance for the H3N2 avian influenza virus.

Avian influenza virus (AIV) is a vital threat to poultry industry and public health. Since wild waterfowl are the natural reservoir of AIV, this virus cannot be easily eliminated (Cheng et al., 2014; Rovida et al., 2017). Furthermore, avian influenza are zoonosis and may cause a global pandemic (Obenauer et al., 2006; Shu and Wang, 2016). Therefore, the trans-species transmission research of AIV is a hot spot of influenza research, especially regarding the molecular mechanism of AIVs effectively adapting to mammalian infection. H3N2 virus circulates in waterfowl in worldwide (Guo et al., 2016; Jonassen and Handeland, 2007; Ramakrishnan et al., 2010). To investigate their genetic adaptation in mammals, we serially passaged a waterfowl-origin H3N2 virus in mice and obtained some mouse-adapted variants. Furthermore, we found eight mutations in these variants: E192K and D701N in PB2 protein; F269S, I475V, and L598P in PB1 protein; V242E in HA protein; G170R in NA protein; and M192V in M1 protein (Yu et al., 2017). Here, we further investigate the effect of these mutations on mammalian pathogenicity and found that both PB2-D701N and M1-M192V mutations could enhance mammalian adaptation and pathogenicity of H3N2 avian influenza virus in mice.

This study was conducted at the biosafety level 3 laboratory in the Military Veterinary Research Institute. All animal experiments were approved by the Review Committee of the Military Veterinary Research Institute. H3N2 parental virus A/baikal teal/Shanghai/SH-89/2013(H3N2) (abbreviated as WT-H3N2) and its mouse-adapted viruses (MA-K1P1, MA-K1P3, MA-K1P7, MA-K1P10, and MA-K1P11) were used in this study. The GenBank accession numbers corresponding to each of the eight WT-H3N2 viral gene segments are KJ907500-KJ907507. H3N2 mouse-adapted viruses (MA-K1P1, MA-K1P3, MA-K1P7, MA-K1P10, and MA-K1P11) were sequenced to identify the adaptive mutations in our previous study (Yu et al., 2017) (Table 1).

The MDCK cell monolayer was infected with H3N2 parent virus WT-H3N2 or its mouse-adapted viruses (MA-K1P1, MA-K1P3, MA-K1P7, MA-K1P10, and MA-K1P11) at a multiplicity of infection (MOI) of 0.01. Cell supernatants were collected at 12, 24, 36, 48, 60, and 72 h after infection and viral titers of the supernatants were determined by end-point titration in MDCK cells. Viral titers were calculated from three replicates by the method of Reed and Muench (1938).

Morbidity and mortality of the H3N2 parent virus or mouse-adapted viruses were analyzed using female 4-6-week-old BALB/c mice (Merial-Vital Laboratory Animal Technology Co., Ltd., Beijing, the People's

* Corresponding author at: Institute of Poultry Science, Shandong Academy of Agricultural Sciences, No. 1 Jiaoxiao Road, Jinan, Shandong, 250023, China.
** Corresponding author at: The Military Veterinary Institute, Academy of Military Medical Science of PLA, 666 Liuyingxi St., Changchun, 130122, China.
E-mail addresses: yuzhijun@shandong.cn (Z. Yu), gaoyuwei@gmail.com (Y. Gao).

https://doi.org/10.1016/j.virusres.2019.06.002
Received 18 January 2019; Received in revised form 17 April 2019; Accepted 2 June 2019
Available online 04 June 2019
0168-1702/

Table 1
MLD_{50} of H3N2 viruses.

Virus[a]	PB2		PB1			HA	NA	M1	MLD_{50}
	192	701	269	475	598	242[b]	170	192	
WT-H3N2	E	D	F	I	L	V	G	M	> 6.5
MA-K1P1	**K**	D	**S**	I	**P**	V	G	M	> 6.5
MA-K1P3	**K**	**N**	**S**	I	**P**	V	G	M	4.5
MA-K1P7	**K**	**N**	**S**	I	**P**	**E**	G	M	4.5
MA-K1P10	**K**	**N**	**S**	**V**	**P**	**E**	**R**	M	4.5
MA-K1P11	**K**	**N**	**S**	**V**	**P**	**E**	**R**	**V**	3.75

[a] WT-H3N2, A/baikal teal/Shanghai/SH-89/2013(H3N2); MA-K1P1, the mouse-adapted virus obtained from the first-generation mice lung; MA-K1P3, mouse-adapted virus obtained from the third-generation mice lung; MA-K1P7, mouse-adapted virus obtained from the seventh-generation mice lung; MA-K1P10 mouse-adapted virus obtained from the tenth-generation mice lung; MA-K1P11, mouse-adapted virus obtained from the eleventh-generation mice lung. These viruses and mutations have been obtained in our previous studies (Yu et al., 2017).

[b] H3 numbering.

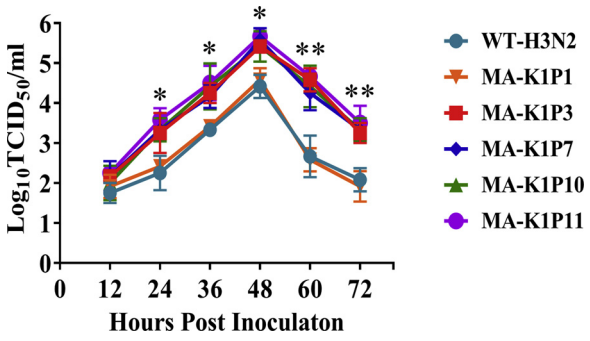

Fig. 1. Growth characteristics of H3N2 viruses *in vitro*. MDCK cells were inoculated at a multiplicity of infection of 0.01 with the WT-H3N2 parental virus or a mouse-adapted virus (MA-K1P1, MA-K1P3, MA-K1P7, MA-K1P10, and MA-K1P11). The average of three experimental replicates is shown with standard deviation indicated using error bars. *, $p < 0.05$, when comparing MA-K1P3 with MA-K1P1 virus, as determined by two-way ANOVA. **, $p < 0.01$, when comparing MA-K1P3 with MA-K1P1 virus, as determined by two-way ANOVA.

Republic of China). Mice were humanely sacrificed when their weight loss > 25% compared to their initial body weight. Mice were intranasally inoculated with 10^5 EID_{50} or 10^4EID_{50} dose of indicated virus. Mouse body weight and death were recorded daily until the fourteenth day after virus challenge. Body weight change and survival represent morbidity and mortality, respectively. The MLD_{50} of the H3N2 subtype of parent virus or mouse-adapted variants was analyzed using groups of females 4–6-week-old BALB/c mice. Mice were intranasally inoculated with 50 µl of 10-fold continuous dilutions from 10^1 EID_{50}/ml to 10^6 EID_{50}/ml of virus in PBS. Mouse body weight and death were recorded daily until the fourteenth day after virus challenge. MLD_{50} were analyzed according to Reed-Muench method (Reed and Muench, 1938).

The lungs' viral titers were detected using female 4-6-week-old BALB/c mice as previous described (Yu et al., 2015). Briefly, animals were intranasally inoculated with 10^6 EID_{50} of indicated virus, and the lungs of three mice were collected in each group at 3 days post inoculation (dpi) and 5 dpi. Viral titers were determined by end-point titration in embryonated eggs and analyzed by the Reed-Muench method (Reed and Muench, 1938). The tissue tropism of H3N2 subtype of parent virus or mouse-adapted viruses were detected using groups of females 4–6-week-old BALB/c mice as previous described (Yu et al., 2015). Briefly, after inoculation with 10^6 EID_{50} of virus, the lungs, brains, livers, spleens, kidneys, and intestines of three mice were collected at 3 dpi. Viral titers were detected by end-point titration in embryonated eggs and analyzed by the Reed-Muench method (Reed and Muench, 1938). All experimental results were analyzed using GraphPad Prism version 5.00.

The effect of these adapted mutations on replication ability *in vitro* were assessed in this study (Fig. 1). Both the MA-K1P1 virus and WT-H3N2 virus possess similar replicated kinetics *in vitro*, indicating that PB2-E192 K, PB1-F269S, and PB1-L598 P cannot change viral replication ability. However, the MA-K1P3 virus replicated faster and brought about higher titers than MA-K1P1 virus (Fig. 1). Furthermore, the MA-K1P3 virus grew to the highest virus titer and yielded about 6.8-fold more virus than MA-K1P1 virus by 48 h post inoculation (hpi) (Fig. 1), indicating that PB2-D701N changed viral replication ability *in vitro*. Lastly, the MA-K1P11, MA-K1P10, or MA-K1P7 virus replicated with similar viral replication kinetics as the MA-K1P3 virus *in vitro* (Fig. 1), indicating that HA-V242E, PB1-I475 V, NA-G170R, and M1-M192V cannot enhanced viral replication *in vitro*. Taken together, our data show that the PB2-D701N mutation can enhance viral replication capacity of H3N2 avian influenza virus.

To analyze the effect of these adapted mutations on virulence of H3N2 subtype of virus in mice, BALB/c mice were infected with 10^5 EID_{50} or 10^4 EID_{50} doses of the parent virus (WT-H3N2) or mouse-adapted viruses (MA-K1P1, MA-K1P3, MA-K1P7, MA-K1P10, and MA-K1P11), respectively. At an infecting dose of 10^5EID_{50}, mice which were inoculated with WT-H3N2 virus or MA-K1P1 virus did not show any body weight loss (Fig. 2A), and all mice survived (Fig. 2B). However, all mice which were infected with MA-K1P3, MA-K1P7, or MA-K1P10 mouse-adapted virus rapidly lost weight and have similar weight loss curve (Fig. 2A), and all mice succumbed to viral infection by day 9 post-infection (Fig. 2B). Furthermore, the MLD_{50} of both WT-H3N2 virus and MA-K1P1 were > 6.5 log_{10} EID_{50}, and the MLD_{50} of MA-K1P3, MA-K1P7, or MA-K1P10 virus were 4.5 log_{10} EID_{50} (Table 1). The MLD_{50} of MA-K1P3 virus was reduced > 100-fold compared to the MA-K1P1 virus. Our results show that PB2-D701N mutation increase mammalian pathogenicity of H3N2 virus in mice and PB2-E192K, PB1-F269S, PB1-I475V, PB1-L598P, HA-V242E, and NA-G170R mutations do not increase the virulence of H3N2 virus in mice. Additionally, at an infecting dose of 10^4EID_{50}, mice which were inoculated with MA-K1P10 virus lost moderate weight (Fig. 2C), and all mice survived (Fig. 2D). However, mice which were inoculated with MA-K1P11 rapidly lost weight (Fig. 2C), and only 2/5 mice recovered from the infection mice (Fig. 2D). Furthermore, the MLD_{50} of MA-K1P11 virus was 3.75 log_{10} EID_{50} (Table 1), indicating that MLD_{50} of MA-K1P11 virus was reduced 5.6-fold compared to the MA-K1P10 virus. Our data indicate that M1-M192V mutation in the context of the other mutations tested increase the mammalian pathogenicity of H3N2 virus. Furthermore, we have tested the effect of M1-M192V alone on viral mammalian pathogenicity by comparing the virulence of an H3N2 virus only possessing M1-M192V mutation with that of parental virus WT-H3N2; however, we found that the MLD_{50} of WT-H3N2-M1-M192V virus was also > 6.5 log_{10} EID_{50}, indicating that there may be no influence of single M1-M192V mutation on the viral mammalian virulence in the context of no other mutations introduced into wide-type H3N2 virus. Additionally, we sequenced the viruses after replication in mice and we did not find additional amino acid changes emerging.

To study the effect of the adaptive mutations on viral replication ability *in vivo,* viral titers of the mice lungs at 3dpi and 5 dpi were assessed (Fig. 3). The MA-K1P1 virus replicated with similar kinetics as the WT-H3N2 virus in lungs, indicating that PB2-E192K, PB1-F269S, and PB1-L598P cannot enhanced viral replication in mice. Lungs' viral titers of MA-K1P1 virus group were 5.50 ± 0.07 log_{10} EID_{50}/g at 3 dpi and 4.96 ± 0.17 log_{10} EID_{50}/g at 5 dpi, respectively (Fig. 3), and Lungs' viral titers of MA-K1P3 virus group were 8.14 ± 0.18 log_{10} EID_{50}/g at 3 dpi and 7.61 ± 0.31 log_{10} EID_{50}/g at 5 dpi, respectively (Fig. 3), these data suggest that PB2-D701N mutation obviously enhance H3N2 AIV replication ability *in vivo*. Lastly, the MA-K1P11, MA-

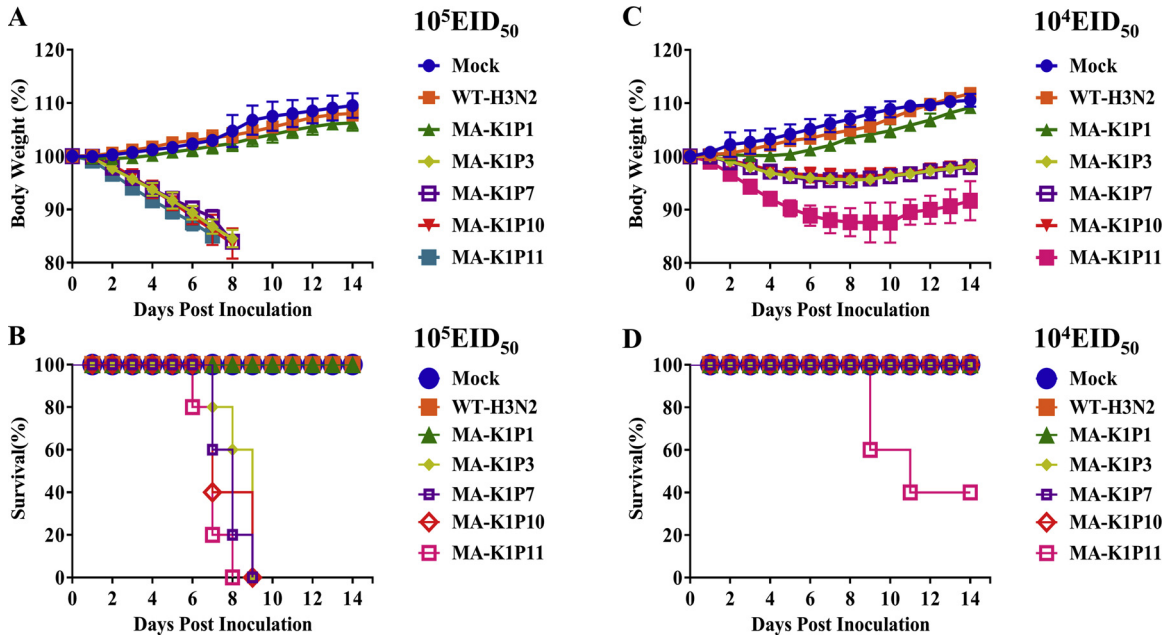

Fig. 2. Morbidity and mortality of H3N2 viruses in mice. (A) Mice (n = 5) were inoculated intranasally with 10^5EID_{50} dose WT-H3N2 parental virus or mouse-adapted variants or mock inoculated (Mock; n = 5). Morbidity is represented as a percentage of the weight on the day of inoculation (day 0). (B) Mortality after inoculation with 10^5EID_{50} dose WT-H3N2 parental virus or mouse-adapted variants or diluent (Mock). (C) Mice (n = 5) were inoculated intranasally with 10^4EID_{50} dose WT-H3N2 parental virus or mouse-adapted variants or mock inoculated (Mock; n = 5). Morbidity is represented as a percentage of the weight on the day of inoculation (day 0). (D) Mortality after inoculation with 10^4EID_{50} dose WT-H3N2 parental virus or mouse-adapted variants or diluent (Mock).

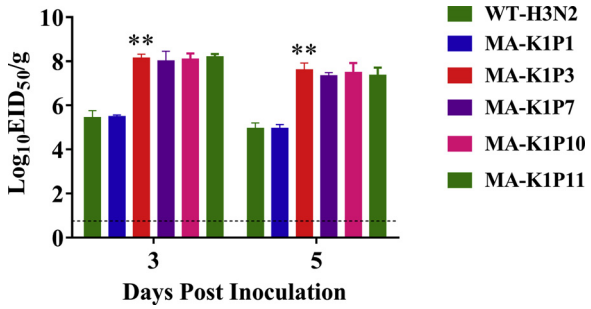

Fig. 3. Growth characteristics of H3N2 viruses *in vivo*. Mice (n = 3) were inoculated intranasally with 10^6 EID_{50} of the parental virus (WT-H3N2) or a mouse-adapted virus (MA-K1P1, MA-K1P3, MA-K1P7, MA-K1P10, and MA-K1P11). Viral titers in the mice lungs were determined at 3 and 5 days post-infection in eggs. The results are expressed as log_{10} EID_{50}/g and the dotted line indicates the limit of detection. The average of three replicates is shown with error bars indicating the standard deviation. **, $p < 0.01$, when comparing MA-K1P3 with MA-K1P1 parental virus, as determined by two-way ANOVA.

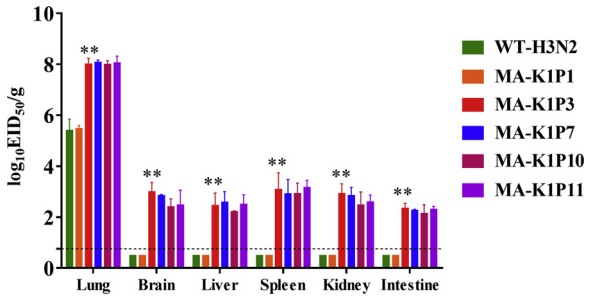

Fig. 4. Viral tissue tropism of H3N2 viruses *in vivo*. Mice (n = 3) were infected with 10^6 EID_{50} of the parental virus (WT-H3N2) or a mouse-adapted virus (MA-K1P1, MA-K1P3, MA-K1P7, MA-K1P10, and MA-K1P11). Lungs, brains, livers, spleens, kidneys, and intestines were collected at day 3 post-infection and viral titers were titrated in eggs. The results are expressed as log_{10} EID_{50}/g and the dotted indicates the lower limit of detection. The average of three replicates is shown with error bars indicating the standard deviation. **, $p < 0.01$, when comparing MA-K1P3 with MA-K1P1 parental virus, as determined by two-way ANOVA.

K1P10, or MA-K1P7 AIV replicated with similar kinetics as the MA-K1P3 AIV in lungs, indicating that HA-V242E, PB1-I475V, NA-G170R, and M1-M192V cannot enhanced viral replication in mice (Fig. 3). Taken together, our results suggest that the PB2-D701N mutation increased mammalian pathogenicity of the H3N2 virus correlates with enhanced viral replication ability *in vivo*.

To assess the influence of the adaptive amino acid substitutions on the viral tissue tropism, mice were inoculated intranasally with 10^6 EID_{50} indicated virus and viral titers of mice organs were detected at 3 dpi (Fig. 4). At the WT-H3N2 virus inoculation group and the MA-K1P1 virus inoculation group, viruses were only detected in the lungs (Fig. 4). However, at the MA-K1P3 virus inoculation group, the MA-K1P7 virus inoculation group, the MA-K1P10 virus inoculation group, and the MA-K1P11 virus inoculation group, viruses were detected in the lungs at higher titers compared to that of the WT-H3N2 virus inoculation group; furthermore, viruses were also detected in the brains, livers, spleens, kidneys, and intestines of mice in these virus inoculation group (Fig. 4).

The above data show that the H3N2 virus possessing a PB2-D701N amino acid substitution could be detected in multiple organs of the infected mice. Our results suggest that PB2-D701N mutation is sufficient to confer H3N2 virus extrapulmonary replication ability in the intestines, brains, kidneys, livers, and spleens of mice.

Avian influenza viruses, unlike other general livestock and poultry pathogens, can spread to humans and threat public health security (He et al., 2016; Hou et al., 2017, 2018; Liu et al., 2009; Wang et al., 2014, 2018; Zhao et al., 2018a,b). The pathogenesis of influenza viruses involves the interaction between virus factors and host factors. The RNA-dependent RNA polymerase of influenza virus consists of PB2, PB1, and PA subunit. The RNA-dependent RNA polymerase mediates viral RNA genome transcription activity and replication activity (Gabriel and Fodor, 2014). In recent years, the viral RNA-dependent RNA polymerase plays a vital role in viral mammalian pathogenicity. Additionally, the viral HA, NP, NA, M1, and NS1 protein also involved in

the virulence of AIV in mammals (Ozawa et al., 2011; Pappas et al., 2008; Smeenk et al., 1996). Here, we found that PB2-D701N and M1-M192V amino acid substitution contribute to the high pathogenicity of H3N2 AIV in BALB/c mice.

In this study, we found that that D701N in PB2 protein enhances viral replication ability and expand viral tissue tropism of H3N2 avian influenza virus, resulting in high virulence of this virus in mammals. PB2 protein has been demonstrated to be a vital pathogenicity determinant of influenza viruses in mammals, and mouse-adapted influenza viruses constantly contain mutations in PB2 gene. The significance of PB2-E627K for mammalian adaptation was first described for an H5N1 virus, and this mutation occurs frequently during the replication of highly pathogenic H5 and H7N9 viruses in mammals (Hatta et al., 2001; Shi et al., 2017). Our data emphasize the major role of the asparagine (N) at position 701 of the PB2 protein for viral pathogenicity of H3N2 avian influenza virus in mice. Residue 701 is located in the 627- nuclear localization signal (NLS) domain of PB2, and it was proposed that PB2-D701N amino acid substitution could destroy the salt bridge between D701 residue and R753 residue and thus expose the NLS and cause enhanced importin-α binding (Gabriel and Fodor, 2014).

M1 is a structural protein that helps mediate viral assembly and interacts with HA and NA and ribonucleoprotein (RNP) (Kamal et al., 2014). Previous studies showed that MA-A41V and M1-T139A were vital pathogenicity determinants for H1N1 virus (Ward, 1995). Additionally, M1-N30D and M1-T215A have been demonstrated to increase the virulence of H5N1 virus in mammals (Fan et al., 2009). However, M1 functional domains are not well understood until now, and the mechanisms of M1 mutations mediating viral pathogenicity variation are still not clear.

Taken together, we found that PB2-D701N and M1-M192V mutation play a role in the virulence variation of H3N2 avian influenza virus in mammals, and researches of viral infection in mammals may parallel or predict the adaptation and pathogenesis of the virus to humans. Lastly, these molecular markers will be of value to future avian influenza and cross-species transmission surveillance.

Conflict of interest

There are no potential conflicts of interest.

Acknowledgements

This work was supported by the Youth Foundation of the Natural Science Foundation of Shandong Province (ZR2018QC005), the National Key Technology R&D Program (2013BAD12B04), National Key Research And Development Plan (2016YFD0500203), National Key Research And Development Plan (2017YFD0500100), the High-Level Talents and Innovative Team Recruitment Program of the Shandong Academy of Agricultural Sciences, High-level Talent Projects (ts201511069; W03020496), and the Construction of Subjects and Teams of Institute of Poultry Science (CXGC2018E11).

References

Cheng, K., Yu, Z., Gao, Y., Xia, X., He, H., Hua, Y., Chai, H., 2014. Experimental infection of dogs with H6N1 avian influenza A virus. Arch. Virol. 159, 2275–2282.
Fan, S., Deng, G., Song, J., Tian, G., Suo, Y., Jiang, Y., Guan, Y., Bu, Z., Kawaoka, Y., Chen, H., 2009. Two amino acid residues in the matrix protein M1 contribute to the virulence difference of H5N1 avian influenza viruses in mice. Virology 384, 28–32.
Gabriel, G., Fodor, E., 2014. Molecular determinants of pathogenicity in the polymerase complex. Curr. Top. Microbiol. Immunol. 385, 35–60.
Guo, X., Flores, C., Munoz-Aguayo, J., Halvorson, D.A., Lauer, D., Cardona, C.J., 2016. Historical and recent cases of H3 influenza a virus in turkeys in Minnesota. Avian Dis. 60, 408.
Hatta, M., Gao, P., Halfmann, P., Kawaoka, Y., 2001. Molecular basis for high virulence of Hong Kong H5N1 influenza A viruses. Science 293, 1840–1842.
He, C.Q., Liu, Y.X., Wang, H.M., Hou, P.L., He, H.B., Ding, N.Z., 2016. New genetic mechanism, origin and population dynamic of bovine ephemeral fever virus. Vet. Microbiol. 182, 50–56.
Hou, P., Wang, H., Zhao, G., He, C., He, H., 2017. Rapid detection of infectious bovine Rhinotracheitis virus using recombinase polymerase amplification assays. BMC Vet. Res. 13, 386.
Hou, P., Zhao, G., He, C., Wang, H., He, H., 2018. Biopanning of polypeptides binding to bovine ephemeral fever virus G1 protein from phage display peptide library. BMC Vet. Res. 14, 3.
Jonassen, C.M., Handeland, K., 2007. Avian influenza virus screening in wild waterfowl in Norway, 2005. Avian Dis. 51, 425–428.
Kamal, R.P., Katz, J.M., York, I.A., 2014. Molecular determinants of influenza virus pathogenesis in mice. Curr. Top. Microbiol. Immunol. 385, 243–274.
Liu, D., Liu, X., Yan, J., Liu, W.J., Gao, G.F., 2009. Interspecies transmission and host restriction of avian H5N1 influenza virus. Sci. China C Life Sci. 52, 428–438.
Obenauer, J.C., Denson, J., Mehta, P.K., Su, X., Mukatira, S., Finkelstein, D.B., Xu, X., Wang, J., Ma, J., Fan, Y., Rakestraw, K.M., Webster, R.G., Hoffmann, E., Krauss, S., Zheng, J., Zhang, Z., Naeve, C.W., 2006. Large-scale sequence analysis of avian influenza isolates. Science 311, 1576–1580.
Ozawa, M., Basnet, S., Burley, L.M., Neumann, G., Hatta, M., Kawaoka, Y., 2011. Impact of amino acid mutations in PB2, PB1-F2, and NS1 on the replication and pathogenicity of pandemic (H1N1) 2009 influenza viruses. J. Virol. 85, 4596–4601.
Pappas, C., Aguilar, P.V., Basler, C.F., Solorzano, A., Zeng, H., Perrone, L.A., Palese, P., Garcia-Sastre, A., Katz, J.M., Tumpey, T.M., 2008. Single gene reassortants identify a critical role for PB1, HA, and NA in the high virulence of the 1918 pandemic influenza virus. Proc. Natl. Acad. Sci. U. S. A. 105, 3064–3069.
Ramakrishnan, M.A., Wang, P., Abin, M., Yang, M., Goyal, S.M., Gramer, M.R., Redig, P., Fuhrman, M.W., Sreevatsan, S., 2010. Triple reassortant swine influenza A (H3N2) virus in waterfowl. Emerg. Infect. Dis. 16, 728–730.
Reed, L.J., Muench, H., 1938. A simple method for estimating fifty percent endpoints. Am. J. Hyg. (Lond.) 27, 493–497.
Rovida, F., Piralla, A., Marzani, F.C., Moreno, A., Campanini, G., Mojoli, F., Pozzi, M., Girello, A., Chiapponi, C., Vezzoli, F., Prati, P., Percivalle, E., Pavan, A., Gramegna, M., Iotti, G.A., Baldanti, F., 2017. Swine influenza A (H1N1) virus (SIV) infection requiring extracorporeal life support in an immunocompetent adult patient with indirect exposure to pigs, Italy, October 2016. Euro Surveill. 22.
Shi, J., Deng, G., Kong, H., Gu, C., Ma, S., Yin, X., Zeng, X., Cui, P., Chen, Y., Yang, H., Wan, X., Wang, X., Liu, L., Chen, P., Jiang, Y., Liu, J., Guan, Y., Suzuki, Y., Li, M., Qu, Z., Guan, L., Zang, J., Gu, W., Han, S., Song, Y., Hu, Y., Wang, Z., Gu, L., Yang, W., Liang, L., Bao, H., Tian, G., Li, Y., Qiao, C., Jiang, L., Li, C., Bu, Z., Chen, H., 2017. H7N9 virulent mutants detected in chickens in China pose an increased threat to humans. Cell Res. 27, 1409–1421.
Shu, Y., Wang, D., 2016. More on probable hospital cluster of H7N9 influenza infection. N. Engl. J. Med. 375, e23.
Smeenk, C.A., Wright, K.E., Burns, B.F., Thaker, A.J., Brown, E.G., 1996. Mutations in the hemagglutinin and matrix genes of a virulent influenza virus variant, A/FM/1/47-MA, control different stages in pathogenesis. Virus Res. 44, 79–95.
Wang, D., Yang, L., Gao, R., Zhang, X., Tan, Y., Wu, A., Zhu, W., Zhou, J., Zou, S., Li, X., Sun, Y., Zhang, Y., Liu, Y., Liu, T., Xiong, Y., Xu, J., Chen, L., Weng, Y., Qi, X., Guo, J., Li, X., Dong, J., Huang, W., Zhang, Y., Dong, L., Zhao, X., Liu, L., Lu, J., Lan, Y., Wei, H., Xin, L., Chen, Y., Xu, C., Chen, T., Zhu, Y., Jiang, T., Feng, Z., Yang, W., Wang, Y., Zhu, H., Guan, Y., Gao, G.F., Li, D., Han, J., Wang, S., Wu, G., Shu, Y., 2014. Genetic tuning of the novel avian influenza A(H7N9) virus during interspecies transmission, China, 2013. Euro Surveill. 19.
Wang, H., Hou, P., Zhao, G., Yu, L., Gao, Y.W., He, H., 2018. Development and evaluation of serotype-specific recombinase polymerase amplification combined with lateral flow dipstick assays for the diagnosis of foot-and-mouth disease virus serotype A, O and Asia1. BMC Vet. Res. 14, 359.
Ward, A.C., 1995. Specific changes in the M1 protein during adaptation of influenza virus to mouse. Arch. Virol. 140, 383–389.
Yu, Z., Cheng, K., Sun, W., Zhang, X., Li, Y., Wang, T., Wang, H., Zhang, Q., Xin, Y., Xue, L., Zhang, K., Huang, J., Yang, S., Qin, C., Wilker, P.R., Yue, D., Chen, H., Gao, Y., Xia, X., 2015. A PB1 T296R substitution enhance polymerase activity and confer a virulent phenotype to a 2009 pandemic H1N1 influenza virus in mice. Virology 486, 180–186.
Yu, Z., Sun, W., Zhang, X., Cheng, K., Zhao, C., Gao, Y., Xia, X., 2017. Multiple amino acid substitutions involved in the virulence enhancement of an H3N2 avian influenza A virus isolated from wild waterfowl in mice. Vet. Microbiol. 207, 36–43.
Zhao, G., Hou, P., Huan, Y., He, C., Wang, H., He, H., 2018a. Development of a recombinase polymerase amplification combined with a lateral flow dipstick assay for rapid detection of the Mycoplasma bovis. BMC Vet. Res. 14, 412.
Zhao, G., Wang, H., Hou, P., He, C., He, H., 2018b. Rapid visual detection of Mycobacterium avium subsp. paratuberculosis by recombinase polymerase amplification combined with a lateral flow dipstick. J. Vet. Sci. 19, 242–250.